

On the Electric Potentials Inside a Charged Soft Hydrated Biological Tissue: Streaming Potential Versus Diffusion Potential

W. Michael Lai

Van C. Mow

Daniel D. Sun

Gerard A. Ateshian

Departments of Mechanical Engineering,
Biomedical Engineering
and Orthopaedic Surgery,
Columbia University,
New York, NY 10027

The main objective of this study is to determine the nature of electric fields inside articular cartilage while accounting for the effects of both streaming potential and diffusion potential. Specifically, we solve two tissue mechano-electrochemical problems using the triphasic theories developed by Lai et al. (1991, ASME J. Biomech. Eng., 113, pp. 245–258) and Gu et al. (1998, ASME J. Biomech. Eng., 120, pp. 169–180) (1) the steady one-dimensional permeation problem; and (2) the transient one-dimensional ramped-displacement, confined-compression, stress-relaxation problem (both in an open circuit condition) so as to be able to calculate the compressive strain, the electric potential, and the fixed charged density (FCD) inside cartilage. Our calculations show that in these two technically important problems, the diffusion potential effects compete against the flow-induced kinetic effects (streaming potential) for dominance of the electric potential inside the tissue. For softer tissues of similar FCD (i.e., lower aggregate modulus), the diffusion potential effects are enhanced when the tissue is being compressed (i.e., increasing its FCD in a nonuniform manner) either by direct compression or by drag-induced compaction; indeed, the diffusion potential effect may dominate over the streaming potential effect. The polarity of the electric potential field is in the same direction of interstitial fluid flow when streaming potential dominates, and in the opposite direction of fluid flow when diffusion potential dominates. For physiologically realistic articular cartilage material parameters, the polarity of electric potential across the tissue on the outside (surface to surface) may be opposite to the polarity across the tissue on the inside (surface to surface). Since the electromechanical signals that chondrocytes perceive in situ are the stresses, strains, pressures and the electric field generated inside the extracellular matrix when the tissue is deformed, the results from this study offer new challenges for the understanding of possible mechanisms that control chondrocyte biosyntheses. [S0148-0731(00)00604-X]

Introduction

A recent focus of articular cartilage research has resulted in many publications on the determination of the effects of mechanical and/or hydrostatic/osmotic pressure loadings on cartilage explant metabolism (e.g., [1–15]). Such studies have been specifically aimed at elucidating possible “mechano-signal” transduction mechanism(s) that might govern the chondrocytes’ biosynthetic activities in maintaining and organizing the large extracellular matrix (ECM) comprising the tissue (see reviews by Comper [16], Mow and Ratcliffe [17], and Muir [18]).¹ Few studies, however, have focused on the details of the fluid and ion flows, and electric potentials *within* the ECM, where chondrocytes reside. Hence, not much is known regarding the exact nature of these signals in the mechano-signal transduction mechanisms that may have stimulated the observed changes in chondrocyte metabolism in these explant studies. The development of more elaborate models of cartilage in recent years allow us to address these mechano-signals that the chondrocytes see *in situ*. Therefore, one aim of this study will be to determine the nature (i.e., magnitude, direction, and time and space variations) of the electric and com-

pression fields within articular cartilage, while accounting for both the streaming potential and the diffusion potential.

The source of all the observed electrical events, measured on the outside surface of articular cartilage derives from the “fixed” negative charges (SO_3^- and COO^-) distributed along the chondroitin, keratan sulfates and hyaluronan molecules comprising the aggrecan *inside* the tissue (e.g., [19–33]). Normally, for the time scale of the electrical events and mechanical deformations considered, these proteoglycans may be assumed to be “immobilized and trapped” inside the ECM, and therefore considered to be fixed to the ECM (e.g., [18,34]). Together with the surrounding collagen network, these proteoglycan macromolecules form the cohesive, strong, porous-permeable, charged, collagen-proteoglycan solid matrix that has been theoretically accounted for in porous media theories such as the biphasic and triphasic theories (e.g., [35,36,17,37]).² For more details on the molecular composition and organization of articular cartilage ECM, see the review chapters in the recent volume on *Extracellular Cellular Matrix*, Harwood Academic Press, Australia, edited by W. D. Comper, 1996 [16].

By virtue of the electro-neutrality law, there is always a cloud of counter-ions (e.g., Ca^{++} , Na^+) and co-ions (e.g., Cl^-) dissolved in the interstitial water surrounding the fixed charges in ECM. At equilibrium, the concentrations of these interstitial ions

¹In this manuscript, “mechano-signal” refers to a combination of mechano-electrochemical events such as stress, strain, pressures (hydrostatic or osmotic), fluid and ion flow, and electrical potential and currents that might simultaneously exist in cartilage when it is deformed.

Contributed by the Bioengineering Division for publication in the JOURNAL OF BIOMECHANICAL ENGINEERING. Manuscript received by the Bioengineering Division June 22, 1999; revised manuscript received February 28, 2000. Associate Technical Editor: L. A. Taber.

²When the effects of the fixed charges are not sought, the biphasic theory of Mow et al. [37] is adequate to describe the deformational behavior of articular cartilage. However, for mechano-electrochemical effects, the triphasic theory should be used, such as the case in this study.

are given by the Donnan equilibrium ion distribution law, which is a statement of the balance between the electrochemical potentials of the ions in the bathing electrolyte solution (e.g., a univalent NaCl of concentration c^*) and those of the ions in the tissue with FCD (c^F) [35,36,38,39]. In general, under the action of driving forces, these ions may move by convection with the interstitial fluid (e.g., due to a hydraulic pressure gradient) or by diffusion through the fluid (e.g., due to a concentration gradient) or by conduction, i.e., drifting through the fluid as a current (due to an electric field). The concentrations of these ions under such nonequilibrium cases can be determined from the laws expressed in the triphasic and multiphase theories.

Motivations

Diffusion Potential in Equilibrium Case. For a given bathing solution of salt concentration c^* , the cation concentration inside the ECM increases with the FCD, whereas the anion concentration decreases with the FCD. In the case where the tissue is equilibrated in a univalent salt bathing solution (e.g., NaCl), the relationships for these changes are given by

$$\frac{dc^+}{dc^F} = \frac{1}{2} \left[1 + \frac{c^F}{\sqrt{(c^F)^2 + 4\gamma^2 c^{*2}}} \right] \quad (1)$$

and

$$\frac{dc^-}{dc^F} = \frac{1}{2} \left[-1 + \frac{c^F}{\sqrt{(c^F)^2 + 4\gamma^2 c^{*2}}} \right] \quad (2)$$

where c^+ , c^- , c^F , c^* , and γ are cation concentration, anion concentration, fixed charge density, external bathing solution salt concentration, and the ratio of activity coefficients of salt, respectively (see derivation of Eqs. (17) and (18) below). Thus, for a tissue with *inhomogeneous* FCD distribution (natural or deformation induced), its FCD gradient will lead to gradients of ion concentrations, with cations and anions having opposite directions for the gradients. As a consequence, there exists a gradient of electric potential inside the tissue, i.e., the diffusion potential, and it is caused by the tendency of the ions to diffuse from a region of higher concentration to a region of lower concentration, thus, causing a slight separation of the positive and the negative charges. The establishment of this diffusion potential opposes the diffusion tendency of the ions. Therefore, there is, in general, even at equilibrium, an electric potential difference between two locations within the tissue if the FCD is nonuniform. Externally, however, the potential difference is zero since the tissue is bathed in one solution.

Diffusion Potential in Nonequilibrium Case. For nonequilibrium cases, it remains true that the cation concentrations increase with the FCD, whereas the anion concentrations decrease with the FCD at every point inside the tissue. However, the laws governing the distributions of ions are more elaborate and must be solved from a set of partial differential equations, including boundary and initial conditions. Therefore, a diffusion potential also exists *inside* the tissue for nonequilibrium cases such as in the permeation and stress relaxation problems. In these nonequilibrium problems, there exists another source of electric potential inside the tissue, the streaming potential, due to movements of ions being convected by interstitial fluid flow. Thus, the main objective of this investigation is to determine the electric potential inside a charged, hydrated and soft biologic tissue, when the effects of both the streaming potential and diffusion potential are considered in these nonequilibrium cases.

A corollary objective of this study is to analyze the nature of the electric potential as would be measured, for example, by Ag/AgCl electrodes placed next to the surface external to the specimen, and compare it with the electric potential immediately inside the specimen. In other words, is the electric potential across the

tissue on the outside different from that across the tissue on the inside. Measurements of electric potential across articular cartilage from the outside have been made by several authors (e.g., [21–30,32]). This electrical phenomenon has been referred to in the literature as the streaming potential since it arises from fluid flow either streaming across the tissue (as in steady permeation) or streaming outward from the tissue (as during a compressive stress-relaxation experiment). The latter phenomenon is also known in the literature as the strain generated potential, i.e., SGP [26].

Phenomenological Transport Theories. All previous studies of electrical events in articular cartilage with the exception of Gu et al. [27] and Lai et al. [40], have used a porous media theory incorporating the classical phenomenological transport equations (see [39,41]) in the *absence* of the diffusion potential. However, due to natural or deformation-induced FCD inhomogeneities, it is the hypothesis of this study that the assumption of no contribution from the diffusion potential is not appropriate for the study of mechano-electrochemical problems in articular cartilage [42]. In previous studies [8,21–23,28], the fluxes were related to the driving forces by the following equation:

$$\mathbf{U} = -k_{11}\nabla P + k_{12}\nabla\psi \quad (3)$$

$$\mathbf{I}_e = k_{21}\nabla P + k_{22}\nabla\psi \quad (4)$$

where \mathbf{U} is the fluid velocity relative to the solid, \mathbf{I}_e is the electric current density, P is fluid pressure, ψ is electric potential, k_{11} is the short circuit hydraulic permeability, k_{22} is the electrical conductivity, and k_{12} and k_{21} are the electrokinetic coupling coefficients. The k_{ij} 's are phenomenological coefficients. The relation between k_{ij} and the physical parameters such as the fixed charge density c^F , molar concentration c_α of the α -ions, the friction coefficients between the ions and the fluid $f_{\alpha w}$, universal gas constant R , absolute temperature T , etc., have been derived by Gu et al. [36]. In that study (i.e., [36]), the following force-flux relationships were derived for the water volume flux \mathbf{J}_w and the electrical current density \mathbf{I}_e in a tissue containing multiple species of ions³:

$$\mathbf{J}_w = -k_o\nabla P - \sum_{\alpha} b_{\alpha} \nabla \left(\frac{RT}{z_{\alpha} F c_{\alpha}} \ln(\gamma_{\alpha} c_{\alpha}) \right) - \chi_o \nabla \psi \quad (5a)$$

$$\mathbf{I}_e = -g_o \nabla P - \sum_{\alpha} g_{\alpha} \nabla \left(\frac{RT}{z_{\alpha} F c_{\alpha}} \ln(\gamma_{\alpha} c_{\alpha}) \right) - \chi_o \nabla \psi \quad (5b)$$

where z_{α} is the valence (including sign, positive for cations and negative for anions), γ_{α} is the activity coefficient for the α -ions, F_c is the Faraday constant, and k_o , b_{α} , g_o , g_{α} , and χ_o are material parameters that are functions of the ion concentrations and the frictional coefficients $f_{\alpha\beta}$ between α and β constituents. On the right hand side of Eq. (5b), the first term ($-g_o\nabla P$) is the convection current, arising from ionic movements due to flow convection under fluid pressure gradient ($-\nabla P$); the second term is the diffusion current, arising from diffusion of ions through interstitial fluid under concentration gradients ($-\nabla c_{\alpha}$), and the last term is the conduction current, arising from ionic movements due to an electric potential gradient ($-\nabla\psi$) which in general includes both induced as well as an externally applied electric field. From this equation, it can be seen that the omission of the diffusion terms in Eqs. (3) and (4) can be justified only if the FCD is uniform at all times. However, for charged hydrated *soft* tissues, the stresses and the strains within the ECM will vary in accordance with the nature of the external loading conditions and with location within the tissue, even if the tissue was initially homogeneous. For example, frictional drag forces associated with fluid permeation will compress the ECM nonuniformly throughout the

³A similar expression for current density can be found in Huyghe and Janssen [43] or Haase [44].

specimen [45,46]. This compaction is most pronounced at the downstream side of the specimen. Also, during a one-dimensional ramped-compression stress relaxation experiment, where the surface is loaded by a free-draining, rigid-porous-permeable loading platen, the ECM will also be compacted in a nonuniform manner; again, the region of highest compaction within the tissue occurs immediately under the loading platen [37,47–50]. As will be demonstrated in this study, these nonuniform compactations have an important effect on the magnitude and polarity of the electric potential inside the tissue.

Driving Forces for the Electric Current Inside the Tissue: Convection Current, Diffusion Current and Conduction Current

According to Eq. (5b), the three driving forces for the electric current inside the tissues are: (1) the mechano-chemical force generated by the gradient of the generalized pressures P , (2) the electro-chemical force generated by the gradient of the concentration c_α (more generally, the activity $a_\alpha = \gamma_\alpha c_\alpha$) for the ionic species, and (3) the electric force generated by the gradient of the electric potential ψ . The generalized pressure P incorporates the hydraulic pressure and the Donnan osmotic pressure effect. In fact, the relationship between gradient of P and the water chemical potential μ^W is given by:

$$\nabla P = \rho_T^W \nabla \mu^W, \quad (6)$$

where

$$\mu^W = \mu_o^W + \left[p - RT \sum \phi_\alpha c_\alpha + B_w e \right] / \rho_T^W. \quad (7)$$

Here p is the hydraulic pressure, c_α is the molar concentration of the α -ion, ϕ_α is the osmotic coefficient for the α -ion, e is the dilatation of the solid matrix, ρ_T^W is the true density of water, B_w is a coupling coefficient, and μ_o^W is the reference chemical potential. The osmotic pressure effect is given by the last two terms within the square brackets on the right side of Eq. (7), where it can be observed that the water chemical potential increases as the ion concentrations decreases and/or matrix dilatation increases (both factors increasing the water concentration). As water is being driven by the mechano-chemical force ∇P , it would convect the ions to flow with it. Since the concentrations of anions and cations are unequal in the charged ECM, this convection would result in an electric current. This is the *convection current* ($-g_\alpha \nabla P$).

According to the concentration term in Eq. (5b), if c_α is non-uniform, diffusion of the ions will take place and thus contribute to the total current. The vector sum of the diffusion movements of each of the ion species is the *diffusion current* ($-\sum g_\alpha (RT/z_\alpha F_c) \nabla \ln(\gamma_\alpha c_\alpha)$).

The electric potential at every point in the tissue is denoted by ψ . This electric potential is the resultant of all the charges in the tissue together with whatever electric and/or magnetic effects the external surroundings might exert on the tissue, including any externally applied electric field. Whenever there is a nonzero gradient of electric potential, it will cause the ions to move, with oppositely charged ions being moved in opposite directions, thus, giving rise to the *conduction current* ($-\chi_o \nabla \psi$).

Electric Field in a Soft Hydrated Tissue With Zero Electric Current

When external circuits are not provided for the tissue to sustain a net charged flow of ions and electrons, the tissue is in a state of zero current. This condition is the most commonly used experimental configuration in the study of charged biological tissues for the determination of their electrical behaviors. For such cases, at every point in the tissue, the sum of the three currents must van-

ish: $\mathbf{I}_e = \text{Convection Current} + \text{Diffusion Current} + \text{Conduction Current} = \mathbf{0}$ or, from Eq. (5b), the gradient of the electric potential becomes:

$$\nabla \psi = \left[-g_o \nabla P + \sum g_\alpha \nabla N_\alpha \right] / \chi_o, \quad (8)$$

where

$$N_\alpha = -(RT/z_\alpha F_c) \nabla \ln(\gamma_\alpha c_\alpha). \quad (9)$$

In this currentless condition, there is no externally applied electric potential, the potential is entirely *induced* by the convection current and the diffusion current. This induced potential generates a conduction current to oppose the convection and diffusion currents so as to achieve the zero current condition. The first term on the right side accounts for the potential induced by convection in the presence of a pressure gradient. This is the *streaming potential*. The second term accounts for the potential induced by the diffusion of ions due to their concentration gradients. These potentials (N_α) are the *diffusion potentials*. In many important experimental configurations, including the steady permeation and the compression stress relaxation problems, the diffusion potential effect competes against the streaming potential effect.

Origin of Diffusion Potential Inside a Charged-Hydrated Biological Tissue With Inhomogeneous FCD

Consider an articular cartilage specimen that is equilibrated in a bathing solution of a univalent salt solution (e.g., NaCl) of concentration c^* . The electro-chemical potentials for the ions inside the tissue are given by [35,36,41]:

$$\bar{\mu}^+ = \bar{\mu}_o^+ + \frac{RT}{M_+} \ln(\gamma_+ c^+) + \frac{F_c \Psi}{M_+}, \quad (10)$$

$$\bar{\mu}^- = \bar{\mu}_o^- + \frac{RT}{M_-} \ln(\gamma_- c^-) - \frac{F_c \psi}{M_-}, \quad (11)$$

where $\bar{\mu}_o^\pm$ are the reference potentials, and M_\pm are the atomic weights. At equilibrium, these potentials are constant inside the tissue and are equal to those in the bath. Thus, Eqs. (10) and (11) yield:

$$\nabla \bar{\mu}^+ = 0 = \frac{RT}{M_+} \nabla \ln(\gamma_+ c^+) + \frac{F_c \nabla \psi}{M_+}, \quad (12)$$

and

$$\nabla \bar{\mu}^- = 0 = \frac{RT}{M_-} \nabla \ln(\gamma_- c^-) - \frac{F_c \nabla \psi}{M_-}, \quad (13)$$

or,

$$\nabla \psi = -\frac{RT}{F_c} \nabla \ln(\gamma_+ c^+) = \frac{RT}{F_c} \nabla \ln(\gamma_- c^-). \quad (14)$$

The electric potential given by Eq. (14) is the diffusion potential. It can be observed that the gradient of electric potential is in the same direction as the gradient of anions and in the opposite direction of the gradient of the cations. This potential opposes the diffusion of the nonuniformly distributed ions caused by the non-uniform FCD in the ECM.

The distribution of the ions in the tissue is given by the Donnan equilibrium distribution law [38], which can be obtained from the equilibrium conditions $\bar{\mu}^+ = \bar{\mu}^{+*}$, $\bar{\mu}^- = \bar{\mu}^{-*}$, and $c^* = c^{+*} = c^{-*}$ (* denoting the external bathing solution). This law is given by the well-known equation:

$$c^+ c^- = \gamma^2 c^{*2}, \quad (15)$$

where c^+ and c^- are related to the FCD (c^F) by the electro-neutrality law:

$$c^+ = c^- + c^F. \quad (16)$$

In Eq. (16), $\gamma = (\gamma_+^* \gamma_-^*) / (\gamma_+ \gamma_-)$ is the ratio of activity coefficients. From Eqs. (15) and (16), the interstitial concentrations for c^+ and c^- may be derived:

$$c^+ = \frac{c^F + \sqrt{(c^F)^2 + 4(\gamma c^*)^2}}{2}, \quad (17)$$

and

$$c^- = \frac{-c^F + \sqrt{(c^F)^2 + 4(\gamma c^*)^2}}{2}. \quad (18)$$

The gradients of c^+ and c^- with respect to c^F yield Eqs. (1) and (2). Clearly, the cation concentration increases with FCD, whereas anion concentration decreases with FCD. As a consequence, the diffusion tendency of the cations and the anions are in opposite directions in a tissue with nonuniform FCD, giving rise to a separation of these oppositely charge ions and inducing a diffusion potential opposing this tendency for separation.

A Special Limiting Case: Rigid Charged Solid Matrix.

Equations (7), (10), and (11) are the chemical potential for water and electro-chemical potentials for cation and anion. Together with the constitutive law for the solid matrix, the mass conservation laws, the equations of motion, the electroneutrality law, and the boundary and initial conditions ([35,36], and also see Appendix A), they comprise the general theory for the transport of water and ions in a charged, hydrated, deformable biological tissue. These nonlinear equations embody many intricate phenomena, and therefore, in general, analytical solutions are not obtainable. However, special cases may be solved to gain insights into some of the complex mechano-electrochemical phenomena in such materials. In this section, the limiting case of a *rigid*, charged, porous-permeable solid matrix, equilibrated in a *dilute* external NaCl bathing solution ($c^*/c^F \ll 1$), is solved to analyze the competition among the three electro-motive forces.

The problem under consideration is a one dimensional steady permeation problem with a hydraulic pressure gradient of ∇p , under an open circuit condition such as in a typical streaming potential experiment (e.g., [27]). Let c_o^F be the FCD distribution within the tissue. For a very dilute solution, the chloride ion concentration is negligible ($c^- \approx 0$) and thus the sodium ion concentration is the same as the FCD to maintain electro-neutrality. That is $c^+ \approx c_o^F$. For the rigid, porous-permeable solid, the solid velocity is zero, i.e., $v^s = 0$. Since $c^- \approx 0$, then under the open circuit condition ($\mathbf{I}_e = \mathbf{0}$), the cation (sodium) velocity v^+ must also be zero. Thus, the momentum equation for the sodium ion takes the form

$$-\rho^+ \frac{d\mu^+}{dz} + f_{w+}(v^w) - F_c \frac{\rho^+}{M_+} \frac{d\psi}{dz} = 0, \quad (19)$$

where μ^+ and ρ^+ are the chemical potential and density of the cation respectively, v^w is the water velocity (a constant for the steady flow case), f_{w+} is the frictional coefficient between the cation and the solvent water and z is the spatial coordinate along the direction of flow (please refer to Appendix A for the governing equations for a triphasic medium). The chemical potential for the cation is given by

$$\mu^+ = \mu_o^+ + \frac{RT}{M_+} \ln(\gamma_+ c^+), \quad (20)$$

where μ_o^+ is the reference chemical potential. Combining Eqs. (19) and (20), together with the relation $\rho^+ = \phi^w c^+ M_+$ yields:

$$\frac{F_c h}{RT} \frac{d\psi}{dz} = \frac{v^w}{D^+/h} - \frac{h}{\gamma_+ c^F} \frac{d}{dz} (\gamma_+ c^F), \quad (21)$$

where $D^+ = (RT \phi^w c^+) / f_{w+}$ is the diffusivity of the cation, and ϕ^w is the volumetric porosity of the tissue (defined on the basis of

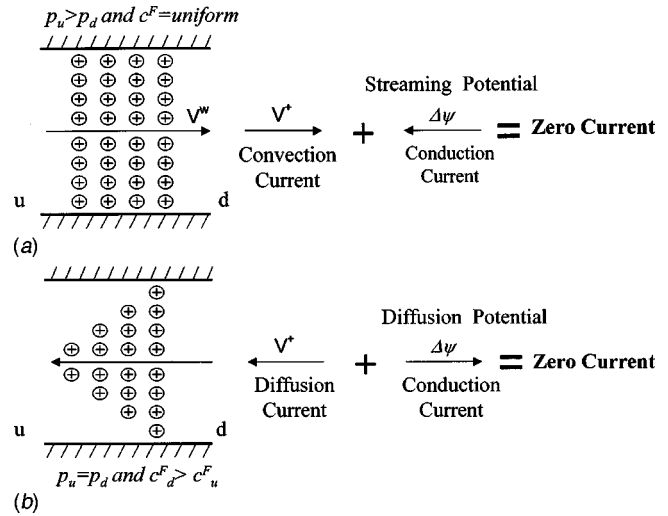


Fig. 1 (a) Schematic diagram to show the flow convection effect on a uniform distribution of cation \oplus corresponding to a uniform distribution of fixed negative charges (not shown). The convection effect causes a convection current, which is countered by the conduction current driven by the streaming potential. (b) Schematic diagram to show the diffusion effect on a nonuniform distribution of cation \oplus corresponding to a nonuniform distribution of fixed negative charges (not shown). The diffusion effect causes a diffusion current, which is countered by the conduction current driven by the diffusion potential.

the extrafibrillar water). If the tissue has a *uniform* FCD, the second term on the right-hand side of Eq. (21) drops out, yielding:

$$\frac{F_c h}{RT} \frac{d\psi}{dz} = \frac{v^w}{D^+/h}. \quad (22)$$

This equation shows a linear electric potential distribution inside the tissue whose slope is proportional to the water velocity and inversely proportional to the cation diffusivity. Note that the potential increases in the direction of v^w , i.e., it increases in the direction of flow. This increase in the downstream direction is due to the fact that the flow convects the positive ion in the downstream direction causing a separation between the positive cation and the stationary negative charges in solid matrix. This streaming potential is always higher in the downstream direction.

A schematic diagram depicting the flow convection effect on a uniform distribution of cation corresponding to a uniform distribution of fixed negative charges (not shown) is presented in Fig. 1(a). The convection effect causes a convection current, which is countered by the conduction current driven by the streaming potential, induced by the slight separation of the positive charges from the fixed negative charges. Note also from the right-hand side of Eq. (22) that this streaming potential is a ratio of two velocities—the velocity of the solvent (v^w) carrying the cation and the characteristic diffusion velocity (D^+/h). A larger solvent velocity enhances the separation and increases the streaming potential. On the other hand, a larger diffusion velocity of the ions diminishes this separation.

The second term on the right-hand side of Eq. (21) shows the effect of a nonuniform distribution of the FCD on the electric potential. If the FCD decreases in the downstream direction, the slope of the potential ($d\psi/dz$) will be enhanced by this term and if the FCD increases in the downstream direction, ($d\psi/dz$) will be reduced by this term. Thus, it is possible that the potential may become negative in the downstream direction if this second term is larger than the first term (the streaming potential term).

The interpretation of this second term is as follows. When FCD increases in the downstream direction, the cation concentration c^+

also increases in the same direction (in this example $c^+ \approx c_o^F$). Therefore, the direction of diffusion of the cation is opposite to the flow, and this diffusion effect tends to separate the cations from the fixed negative charges in a direction opposite to that due to the streaming effect. Thus, the diffusion potential here impedes the streaming potential. If FCD decreases in the downstream direction, then both the streaming potential and the diffusion potential will reinforce each other. A schematic diagram depicting this diffusion effect is shown in Fig. 1(b). Here, the diffusion effect is countered by the conduction current driven by the diffusion potential.

The assumptions of rigid matrix and very dilute solution have enabled us to obtain a simple analytical equation that provides us with a clearer understanding of the two mechanisms causing the electric potential within such a material. However, for *soft* tissues such as the articular cartilage, intervertebral disk, growth plate, cornea, etc., deformation of the tissue generally is not negligible. When a deformable tissue is under the same steady filtration condition, flow induced compaction will occur (e.g., [27,45,46]). For a tissue with initially homogeneous properties, the drag-induced compaction is nonuniform, increasing monotonically in the downstream direction. As a consequence, under the steady filtration condition, FCD will increase in the downstream direction due to this flow-induced compaction. Thus, for such tissues, both streaming potential and diffusion potential must always exist inside the tissue and in fact they always compete against each other.

Electric Potentials Across the Tissue: Outside Versus Inside. Thus far, the discussion has focused on the distribution of electric potential *inside* the tissue. Since there are always two sides to each boundary surface, one facing the external bath and the other facing inside the tissue, it is necessary to be specific when referring to the potential across the tissue. The electric potentials across the tissue in any experiment are measured from the outside, while chondrocytes always experience the electric potential on the *inside*. The question may be asked: Are the externally measured electric potentials an accurate indication of the internal electric potentials? As will be shown, the answer is that these two potentials are in general different.

Let a sample tissue layer be bounded between $z=0$ and $z=h$, with external baths defined in the domain $z<0$ and $z>h$. Let $\psi^*(0)$ and $c^{+*}(0)$ be the electric potential and cation concentration respectively in the bath side $z=0^-$, and let $\psi(0)$ and $c^+(0)$ be the corresponding values inside the tissue at the same surface (i.e., $z=0^+$). Similar notations are defined for the boundary at $z=h^+$: $\psi^*(h)$, $c^{+*}(h)$ and at $z=h^-$: $\psi(h)$ and $c^+(h)$. Then, the continuity condition on the electrochemical potential across the boundaries for the cation yields:

$$\psi^*(0) - \psi(0) = \frac{RT}{F_c} \ln \frac{a^+(0)}{a^{+*}(0)}, \quad (23a)$$

$$\psi^*(h) - \psi(h) = \frac{RT}{F_c} \ln \frac{a^+(h)}{a^{+*}(h)}. \quad (23b)$$

Here $a^+ = \gamma_+ c^+$ and $a^{+*} = \gamma_+^* c^{+*}$ are the activities. From these equations, it can be easily obtained that the difference between the measured external electric potential $[\psi^*(h) - \psi^*(0)]$ at the surface across the tissue, and the internal electric potential $[\psi(h) - \psi(0)]$ at the surface across the tissue, is given below:

$$\psi^*(h) - \psi^*(0) = [\psi(h) - \psi(0)] + \frac{RT}{F_c} \ln \frac{a^+(h)a^{+*}(0)}{a^{+*}(h)a^+(0)}. \quad (24)$$

Thus, in general, the outside electric potential across the tissue will be different from the inside potential across the tissue. Clearly, they will be the same if and only if

$$\frac{a^+(h)}{a^{+*}(h)} = \frac{a^+(0)}{a^{+*}(0)}. \quad (25)$$

If the upstream bath and the downstream bath are kept at the same ionic condition (a commonly assumed condition in streaming potential experiments), then $a^{+*}(0) = a^{+*}(h)$ and we have

$$\psi^*(h) - \psi^*(0) = [\psi(h) - \psi(0)] + \frac{RT}{F_c} \ln \frac{a^+(h)}{a^+(0)}. \quad (26)$$

In a one-dimensional filtration experiment, for an initially homogeneous tissue, due to flow induced compaction, the cation concentration on the downstream side $c^+(h)$ will always be larger than $c^+(0)$ on the upstream side *inside* the tissue. Therefore, assuming that the ratio of activity coefficients is unity, the logarithmic term on the right-hand side of Eq. (26) is positive, while the first term of this equation can be either positive or negative. It will be negative if the tissue is sufficiently soft so that the diffusion potential dominates over the streaming potential. Therefore, in general, the electric potential across the tissue as measured from *outside* may be different (even in sign, when the diffusion potential dominates) than the electric potential from the *inside*.

Electrochemical Potential Versus Electric Potential Across the Tissue. Ag/AgCl electrodes are often used to measure the electric potential across a tissue specimen on the outside in the permeation experiment, and in stress-relaxation and creep experiments. It is known that, in experiments where one single salt, such as NaCl is involved, such electrodes measure a constant multiple of the *electrochemical potential* of the anions (Cl^-) across the tissue [41], which is not necessarily the same as the *electric potential* across the tissue. Indeed, from Eq. (11), the relationship between these two potentials is given by:

$$-\frac{M_-}{F_c} [\bar{\mu}^{-*}(h) - \bar{\mu}^{-*}(0)] + \frac{RT}{F_c} \ln \frac{a^{-*}(h)}{a^{-*}(0)} = [\psi^*(h) - \psi^*(0)], \quad (27)$$

where $a^{-*} = \gamma_-^* c^{-*}$. The first term on the left-hand side of Eq. (27) is what the electrodes measure, and it differs from the electric potential across the tissue if the logarithmic term is not zero. In a steady permeation experiment, if the ionic conditions in the upstream and downstream baths are kept the same, the logarithmic term is zero, so that across the tissue the measured value (using Ag/AgCl electrodes) is indeed the desired electric potential and it is directly proportional (with proportional constant M_-/F_c) to the negative of the electrochemical potential. In other experimental configurations (stress relaxation, creep, etc.), the same may not always hold, depending on the experimental boundary conditions.

Steady Permeation of NaCl Solution Through a Layer of Articular Cartilage. A schematic diagram for electromechanical one-dimensional permeation experiment on articular cartilage is shown in Fig. 2. The layer of tissue is supported by a rigid porous-permeable, free-draining platen at its downstream side ($z=0$). A NaCl solution of concentration c^* is forced through the tissue layer of thickness h , under a pressure drop $\Delta p^* = p_u^* - p_d^*$ across the tissue (p_u^* and p_d^* are upstream and downstream hydraulic pressures with $p_u^* > p_d^*$, i.e., the flow is from left to right). The boundary conditions for this problem are:

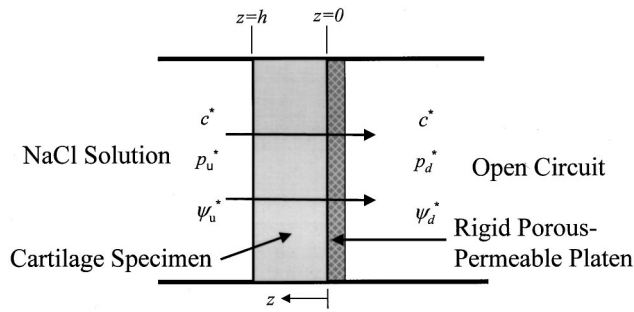
$$\mu^s(0) = 0, \quad \mu^W(0) = \mu_d^{W*}, \quad \bar{\mu}^\pm(0) = \bar{\mu}_d^{\pm*}, \quad (28)$$

at $z=0$ (downstream),

and

$$\sigma_z(h) = -p_u^*, \quad \mu^W(h) = \mu_u^{W*}, \quad \bar{\mu}^\pm(h) = \bar{\mu}_u^{\pm*}, \quad (29)$$

at $z=h$ (upstream).



$$\begin{aligned} \sigma_z(h) &= -p_u^*, & \mu^w(h) &= \mu_u^{w*}, & \tilde{\mu}^\pm(h) &= \tilde{\mu}_u^{\pm*} \\ u^s(0) &= 0, & \mu^w(0) &= \mu_d^{w*}, & \tilde{\mu}^\pm(0) &= \tilde{\mu}_d^{\pm*} \end{aligned}$$

Fig. 2 Schematic of open circuit one-dimensional permeation experiment with the upstream pressure greater than the downstream pressure ($p_u^* > p_d^*$); flow is from left to right

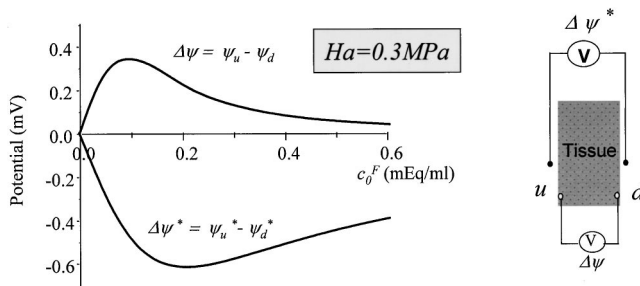


Fig. 3 Steady permeation: electric potential across the tissue from the *inside* ($\Delta\psi$), and electric potential across the tissue from the *outside* ($\Delta\psi^*$), as a function of initial fixed charge density. For $H_a=0.3$ MPa, the diffusion potential dominates over streaming potential. ($D^+=0.5 \times 10^{-9}$ m²/s, $D^-=0.8 \times 10^{-9}$ m²/s, $K=7 \times 10^{14}$ Ns/m⁴, $\phi_o^w=0.80$, $c^+=0.15$ M, $\Delta p=30$ KPa).

Here σ_z , the total mixture stress, is the imposed pressure. These boundary conditions express that the total stress, the chemical potential, and the electrochemical potential are continuous across the boundaries and that the porous-permeable platen at $z=0$ is rigid.

In the common permeation problem (e.g., [27]), the upstream bath and the downstream bath have the same NaCl concentration c^* . Also, in these experiments, an ‘‘open circuit’’ condition is imposed. Under the steady flow condition, the solid matrix velocity is zero; therefore the currentless condition is:

$$c^+ v^+ = c^- v^- \quad (30)$$

The governing nonlinear equations for a triphasic medium (see Appendix A) together with the boundary conditions above are solved using the finite element method developed by Sun et al. [51] and the results have been checked with a finite difference method. The electric potentials across the tissue (inside to inside as well as outside to outside) as a function of the initial uniform FCD are shown in Figs. 3 and 4. The potential across the tissue from the *inside* is denoted as $\Delta\psi$, and that across the tissue from the *outside* is denoted as $\Delta\psi^*$. All material parameters (diffusivities D^+ and D^- , diffusive resistance coefficient between interstitial water and solid matrix K , the initial porosity ϕ_o^w , the NaCl concentration c^* , and the pressure drop Δp^*) are the same for both Figs. 3 and 4, except the intrinsic solid matrix triphasic aggregate modulus H_a .⁴ In Fig. 3 (softer tissue with H_a

⁴The relation between the triphasic H_a and the biphasic H_A and Donnan osmotic pressure is given in Appendix B.

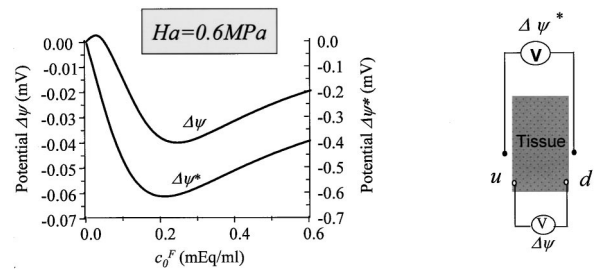


Fig. 4 Steady permeation: electric potential across the tissue from the *inside* ($\Delta\psi$), and electric potential across the tissue from the *outside* ($\Delta\psi^*$), as a function of the initial fixed charge density. For $H_a=0.60$ MPa, the streaming potential effect dominates over the diffusion potential effect, except for a region of low FCD. Other parameters same as in Fig. 3.

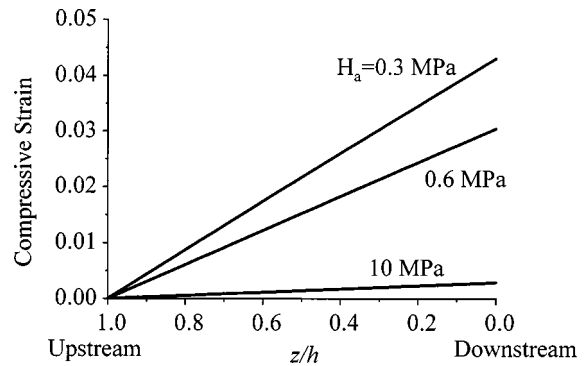


Fig. 5 Steady permeation: compressive strain inside the tissue for three values of H_a . The strain is caused by frictional force of permeation between water and solid matrix. The strain increases monotonically in the downstream direction. ($c_o^F=0.2$ mEq/ml, other parameters same as in Fig. 3).

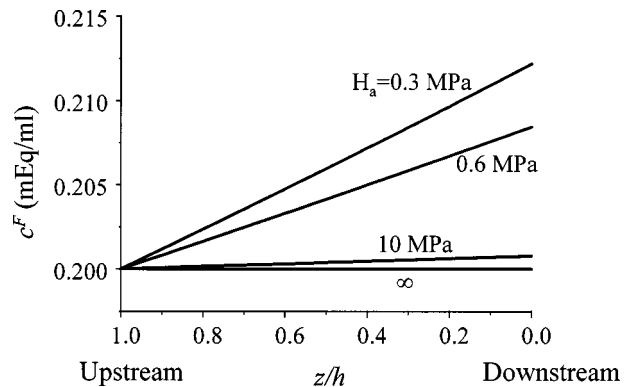


Fig. 6 Steady permeation: fixed charge density increases in the downstream direction due to drag-induced compaction (see Fig. 5)

=0.3 MPa), $\Delta\psi^*$ and $\Delta\psi$ are of opposite polarity, whereas in Fig. 4 (stiffer tissue with $H_a=0.6$ MPa), the two potentials are generally of the same polarity. Again, this difference in response is due to the competition between the convection effect (i.e., streaming potential) and the diffusion effect (i.e., diffusion potential). Softer tissues will experience a larger drag-induced compaction effect than stiffer tissues; the drag-induced compaction and change of FCD inside the tissue are shown in Figs. 5 and 6, respectively. Clearly, in the limiting case of a rigid matrix, the FCD is unchanged from the initial uniform value.

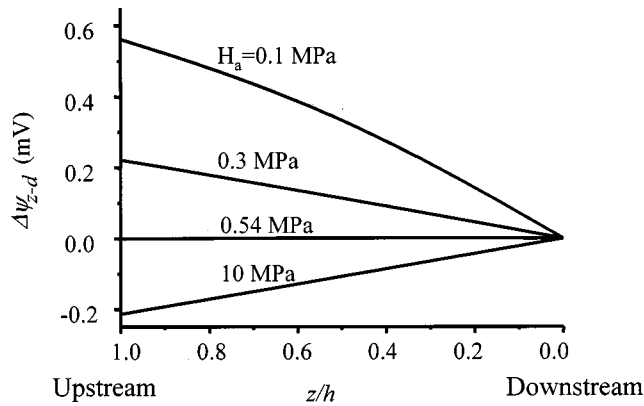


Fig. 7 Steady permeation: electric potential distribution inside the tissue for four values of aggregate modulus. Again, the diffusion potential dominates over the streaming potential for tissues with small aggregate modulus, the reverse is true for tissues with larger aggregate modulus (same parameter values as in Fig. 5).

The distribution of the electric potential inside the tissue for four values of the triphasic aggregate modulus H_a is presented in Fig. 7. It can be observed that the internal electric field changes its polarity at approximately $H_a = 0.54$ MPa, indicating that the streaming effect will dominate inside the tissue when $H_a > 0.54$ MPa. In this case, the electric potential is more positive *downstream*. On the other hand for $H_a < 0.54$ MPa, the drag-induced compaction will cause the diffusion potential to dominate the electric potential inside the tissue. In this case, the electric potential is more positive *upstream*. Note also that the curvature of the distribution is related to the induced electric dipoles in the medium [52]. Clearly, these results demonstrate that what electric potential (magnitude and polarity) that the chondrocytes will see *in situ* depends on the aggregate modulus of articular cartilage, and their location within the tissue.

Electric Field in Confined Compression Stress Relaxation Experiment. A schematic diagram for a one-dimensional ramped displacement relaxation experiment is shown in Fig. 8. The layer of tissue is confined within a rigid-cylindrical container whose side-wall and bottom are insulated against flow of water and ions. On its top is a rigid porous-permeable loading platen. The ramped-displacement imposed on this loading platen is given in Fig. 8(b). In addition to the stress relaxation, the transient response of the electric potential distribution is to be determined. It

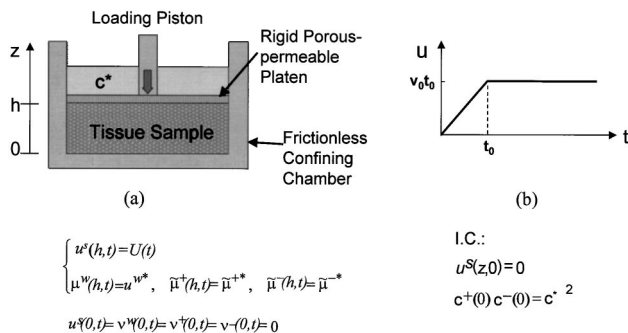


Fig. 8 (a) Schematic of an open-circuit, one dimensional ramped-displacement, stress-relaxation experiment. The bathing solution NaCl concentration c^* is kept fixed during the experiment, and the motion of the loading piston is prescribed in (b). The surface to surface strain is -0.1 , $t_o = 200$ s and $h = 2$ mm.

will be assumed that the tissue is initially equilibrated in a NaCl solution of concentration c^* . The friction between the container and the tissue will be neglected. The boundary conditions for this problem are given by:

$$u^s(0, t) = 0, v^w(0, t) = v^+(0, t) = v^-(0, t) = 0, \text{ at } z = 0, \quad (31)$$

and

$$u^s(h, t) = U(t), \mu^w(h, t) = \mu^{w*}, \bar{\mu}^+(h, t) = \bar{\mu}^{+*}, \text{ at } z = h. \quad (32)$$

Here $U(t)$ is the imposed ramped displacement function, i.e.,

$$U(t) = v_o t \quad \text{for } t \leq t_o, \\ U(t) = v_o t_o \quad \text{for } t \geq t_o \quad (33)$$

The initial conditions for this problem are:

$$u^s(z, 0) = 0, \quad (34)$$

and

$$c^+(z, 0) c^-(z, 0) = \gamma_{\pm}^2 c^{*2}. \quad (35)$$

This last condition expresses the Donnan equilibrium ion distribution prior to the application of the ramped-displacement $U(t)$. The experiment is again ‘‘open circuit,’’ and in this problem where $v^s \neq 0$, the currentless condition is expressed as

$$c^+(v^+ - v^s) = c^-(v^- - v^s). \quad (36)$$

The transient mechanical response for this relaxation problem has been recently published [50]. The transient response of the electric field has now also been obtained, and is presented below.

The electric potential distribution $\Delta\psi_{z-B}[\psi(z, t) - \psi(0, t)]$ inside the tissue for the stress relaxation problem (at various times) is shown in Fig. 9. This case ($H_a = 0.3$ MPa) illustrates the domination of the diffusion potential over the streaming potential. It is seen here that $\Delta\psi_{z-B}$ is negative for all times, that is $\psi(0, t) \geq \psi(z, t)$ so that the electric potential increases from porous platen toward the bottom of the container. This strain generated electric potential inside the tissue has an opposite polarity to the (electrochemical) potential reported in the literature from Ag/AgCl measurements taken outside the tissue [26]. This large diffusion potential effect is due to the compaction of the charged solid matrix during the ramp phase of the experiment. The variations of the compressive strain with time and depth are shown in Fig. 10. Clearly, higher compaction and higher FCD are seen near

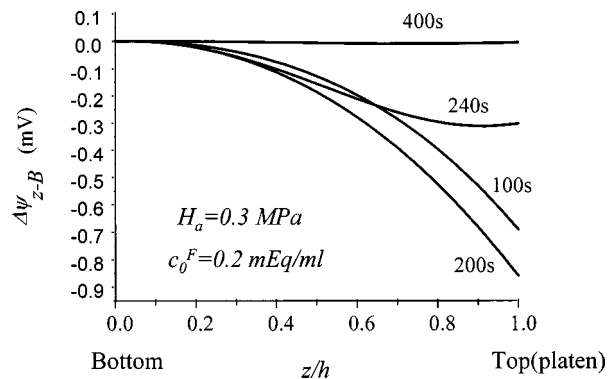


Fig. 9 Stress relaxation: electric potential distribution inside the tissue at various times for $H_a = 0.3$ MPa. The potential increases in the direction toward the bottom indicating that it is dominated by the diffusion potential effect. Fluid flow is in the upward direction into the porous-permeable, loading-platen during the entire compression phase. ($c_o^F = 0.2$ mEq/ml, other parameters same as in Fig. 3).

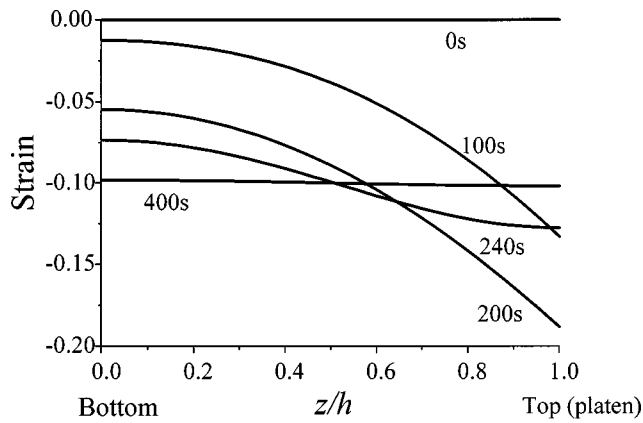


Fig. 10 Stress relaxation: compressive strain distribution inside the tissue at various times. The nonuniformity of the strain is caused by frictional drag force of permeation between water and solid matrix. The strain increases monotonically in the upward (flow) direction.

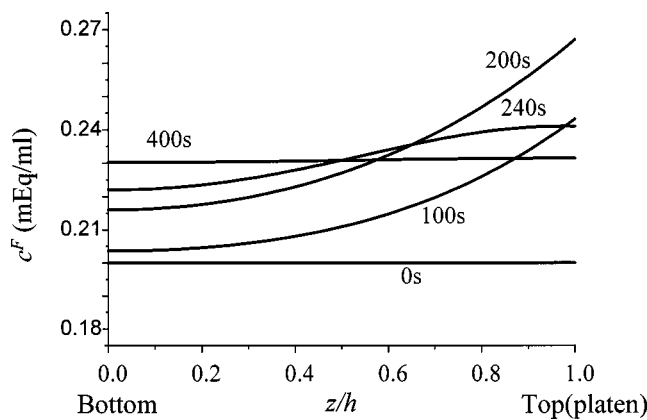


Fig. 11 Stress relaxation: FCD distribution caused by the drag-induced compaction (see Fig. 10)

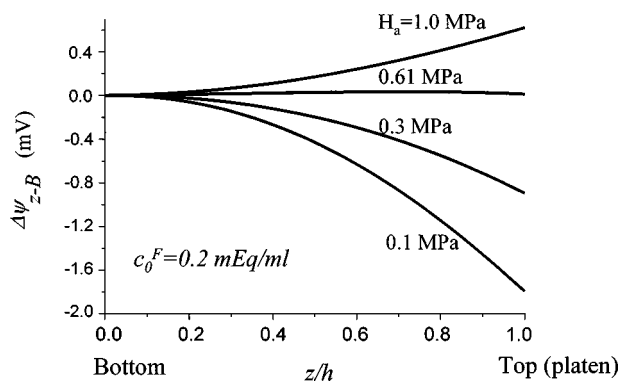


Fig. 12 Stress relaxation: electric potential distribution inside the tissue at time $t=200$ s (i.e., at the end of the compression-ramp phase) for four values of aggregate modulus. For more rigid tissue ($H_a > 0.61$ MPa), the streaming potential effect dominates whereas for softer tissues ($H_a < 0.61$ MPa), the diffusion potential effect dominates. ($c_0^F = 0.2$ mEq/ml, other parameters same as in Fig. 3).

the porous platen (on top) (Figs. 10 and 11). Thus, for this case ($H_a = 0.3$ MPa), the diffusion potential effect dominates over the streaming potential effect.

For tissues with larger compressive stiffness, the opposite may be true, i.e., the streaming potential dominates with more positive

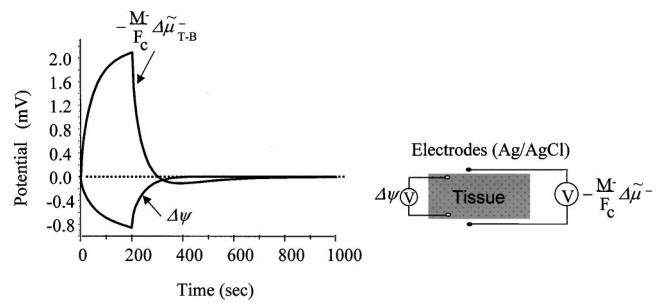


Fig. 13 Stress relaxation: electric potential across the tissue from the inside ($\Delta\psi$) and the electrochemical potential for anion across the tissue ($\Delta\mu^-$). Note: Ag/AgCl electrodes measure the electrochemical potentials ($-M_-/F_c$) $\Delta\mu^-$.

potential near the porous-permeable loading platen. The electric potential for four values of aggregate modulus H_a are shown in Fig. 12. The results show that the electric fields inside the tissue reverse its polarity at approximately $H_a = 0.61$ MPa.

The electric potential $\Delta\psi$ across the tissue on the inside is shown in the bottom curve of Fig. 13. Also shown in the figure is the electrochemical potential measured across the tissue on the outside. This potential (including the proportional constant (M_-/F_c) is what the Ag/AgCl electrodes measure across the tissue on the outside [41]. Thus, the polarity of the electrochemical potential measured by the electrodes on the outside can be opposite to that of the electric potential across the tissue on the inside for soft tissues. This may be the case, for example, for osteoarthritic cartilage when it experiences significant softening during the disease process [53].

Discussion and Conclusions

The importance of the diffusion potential relative to the streaming potential in charged, hydrated, soft biological tissues has been examined in this study in two well-known experimental configurations: (1) the one-dimensional steady permeation experiment, and (2) the one-dimensional ramped-displacement, compression, stress-relaxation experiment. In these two problems, it was found that under an open circuit condition where the sum of the streaming current, diffusion current, and conduction current is zero, the streaming current (inducing streaming potential) and the diffusion current (inducing the diffusion potential) are in opposite directions. Thus, the magnitude and polarity of the resulting electric potential depend on the relative magnitudes of these two effects. The streaming potential arises from the slight separation of the bulk of the positive charges from that of the negative charges due to the flow convection effects caused by a pressure gradient (hydraulic and/or osmotic). The diffusion potential arises from the slight separation of the bulk of positive charges from that of the negative charges due to diffusion caused by the gradients of mobile ions in the presence of a FCD gradient. The nonuniform distribution of FCD may be natural as is the case in articular cartilage (see, e.g., [32]), or may be due to flow-induced compaction or compression [46,49,50]. Only if the FCD is uniform does the diffusion potential vanish. Therefore, for studies of the mechano-electrochemical responses of articular cartilage, the existence of a diffusion potential should not be neglected since cartilage FCD is in general nonuniform (intrinsic and/or induced by matrix deformation).

The results from this study also clarify the meaning of the electric potential measured using Ag/AgCl electrodes. In any one-dimensional problem with bathing solutions on its two ends, the measured electrochemical potential across the two outside baths is in general not the electric potential. It is the electric potential if both bathing solutions contain identical electrolytes and concentrations. Also results from this study show that, in general, the

electric potential across the tissue on the *outside* is not the same as the electric potential *inside* the tissue. They may be the same if the matrix is rigid and with uniform FCD. Thus, care must be exercised in extrapolating from the measured electrochemical data outside of the tissue to those electric events occurring inside the tissue. Furthermore, inasmuch as Ag/AgCl electrodes measure *electrochemical* potential of Cl^- , which is continuous across the tissue boundary (not the *electric* potential), simply placing these electrodes inside the tissue will not measure potential difference across the tissue any different from that measure from outside. Indeed, similar to the Donnan potential problem, experimental measurements of this potential poses a challenging problem [54]. Finally, again, since it is believed that electrical events inside the tissue are important in stimulating chondrocyte biosyntheses (see, e.g., [6,8]), the effects of the diffusion potential should be taken into consideration to determine the electrical events within the ECM.

In addition to the nonuniform distribution of the FCD in articular cartilage, the electrical effects due to the diffusion potential may become even more important when a tissue is softened during a disease process such as osteoarthritis [17,32,53]. For the realistic physical parameters considered in this study, it has been shown that when H_a is less than approximately 0.6 MPa, the diffusion potential effect will dominate over the streaming potential effect significantly by modulating the magnitude and/or reversing the polarity of the electric potential. In osteoarthritic cartilage, with matrix degradation, the intrinsic compressive stiffness always diminishes, thus affecting chondrocyte deformation and metabolic activities (e.g., [1,3,6,14,15,55]) as well as the nature of the mechano-electrochemical events within cartilage when it is deformed.

In summary, the triphasic theory is used to study convection as well as diffusion effects in a charged hydrated soft tissue. It has been found that the competition of streaming potential and diffusion potential offers possible new ways to interpret the challenging data that have been produced from cartilage explants studies attempting to understand the mechano-signal transduction mechanisms controlling chondrocyte biosynthesis.

Acknowledgement

This work was supported by NIH Grants No. AR41913 and No. AR42850.

Nomenclature

$a^+, a^- (a^{+*}, a^{-*})$	= ionic activities (*=in bath)
B_w	= coupling material coefficient in water
b_α	= chemical potential
b_α	= coupling coefficient
c^*	= NaCl concentration in bath
$c^\pm (c^{\pm*})$	= molar concentrations of anion and cation inside tissue (*=in bath)
$c^F (c_o^F)$	= fixed charge density (o =reference value)
D^\pm	= diffusivities of anion and cation
e	= tissue dilatation
F_c	= Faraday constant
$f_{\alpha\beta}$	= frictional coefficient between α and β species
g_o, g_α	= ionic conductivities
H_A	= biphasic aggregate modulus
H_a	= triphasic aggregate modulus
h	= thickness of the tissue layer
I_e	= electric current density
J_v	= water volume flux
k_o	= hydraulic permeability
M_\pm	= atomic weight of the ionic species
N_α	= diffusion potential
P	= generalized pressure
p	= water pressure

$p_u(p_d)$	= water pressure at upstream site (subscript d =downstream site)
R	= universal gas constant
T	= absolute temperature
z_α	= valence for the α ion (including sign)
u^s	= displacement of solid phase
v^S	= velocity of the solid phase
v^W	= velocity of the interstitial water phase
v^\pm	= velocities of the ionic species
ϵ	= one-dimensional strain relative to configuration at bath concentration c^*
$\psi(\psi^*)$	= electric potential inside the tissue (in bath)
ρ_T^W	= true density of pure water
ρ^α	= apparent densities ($\alpha=s, w, +, -$)
$\tilde{\mu}^\pm(\tilde{\mu}^{\pm*})$	= electrochemical potentials for ions inside tissue (superscript *=in bath)
$\mu^\pm(\mu^{\pm*})$	= chemical potentials for ions inside tissue (superscript *=in bath)
$\mu^W, (\mu^{W*})$	= water chemical potential in tissue (superscript *=in bath)
ϕ_α	= osmotic coefficients for the α ion
γ_α	= activity coefficient for the α ion
γ	= γ_\pm^*/γ_\pm
$\gamma_\pm(\gamma_\pm^*)$	= mean activity coefficient for the ions (*=in bath)
$\phi^W(\phi_o^W)$	= porosity (initial value)
χ_o	= $\sum g_\alpha$ =tissue conductivity
$\sigma(\sigma_z)$	= mixture stress (normal stress on z plane)

Appendix A

Governing Equations for a Triphasic Medium. (see nomenclature for definition of the symbols)

(I) *Momentum Equations (Quasi-static):*

$$\text{Water: } -\rho^W \nabla \mu^W + f_{sW}(\mathbf{v}^S - \mathbf{v}^W) + f_{+W}(\mathbf{v}^+ - \mathbf{v}^W) + f_{-W}(\mathbf{v}^- - \mathbf{v}^W) = 0, \quad (\text{A1.1})$$

$$\text{Cation: } -\rho^+ \nabla \tilde{\mu}^+ + f_{s+}(\mathbf{v}^S - \mathbf{v}^+) + f_{+W}(\mathbf{v}^W - \mathbf{v}^+) + f_{-+}(\mathbf{v}^- - \mathbf{v}^+) = 0, \quad (\text{A1.2})$$

$$\text{Anion: } -\rho^- \nabla \tilde{\mu}^- + f_{s-}(\mathbf{v}^S - \mathbf{v}^-) + f_{-W}(\mathbf{v}^W - \mathbf{v}^-) + f_{+-}(\mathbf{v}^+ - \mathbf{v}^-) = 0, \quad (\text{A1.3})$$

$$\text{Tissue: } \text{div } \sigma = 0. \quad (\text{A1.4})$$

where $f_{\alpha\beta} = f_{\beta\alpha}$. In this paper f_{+-} , f_{s+} , and f_{s-} are assumed to be negligible.

(II) *Electroneutrality Condition:*

$$c^- + c^F = c^+ \quad (\text{A2})$$

(III) *Continuity Equations:*

$$\frac{\partial \rho^\alpha}{\partial t} + \text{div}(\rho^\alpha \mathbf{v}^\alpha) = 0 \quad (\text{A3})$$

(IV) *Constitutive Equations:*

$$\mu^w = \mu_o^w + \frac{1}{\rho_T} [p - RT\phi(c^+ + c^- + c^F) + B_w \text{tr} \mathbf{E}], \quad (\text{A4.1})$$

$$\tilde{\mu}^+ = \tilde{\mu}_o^+ + \frac{RT}{M_+} \ln(\gamma_+ c^+) + \frac{F_c \psi}{M_+}, \quad (\text{A4.2})$$

$$\bar{\mu}^- = \bar{\mu}_o^- + \frac{RT}{M_-} \ln(\gamma_- c^-) - \frac{F_c \psi}{M_-} \quad (A4.3)$$

$$\sigma = -p\mathbf{I} + \lambda_s \text{tr}(\mathbf{E}) + 2\mu_s \mathbf{E} \quad (A4.4)$$

(V) Conservation of Fixed Charges:

$$\frac{\partial c^F}{\partial t} + \text{div}(c^F \mathbf{v}^s) = 0 \quad (A5)$$

Appendix B

Relationship Between H_A and H_a . In the one-dimensional configuration,

$$\sigma = -p + H_a \frac{du}{dz}, \quad (B1)$$

where σ is the mixture stress, p is pressure, $H_a = \lambda_s + 2\mu_s$ is the triphasic aggregate modulus, u is the solid matrix displacement measured from the hypertonic configuration. Let $u'(z)$ be the free swelling displacement, at bath concentration c^* (e.g., 0.15 M NaCl), measured from the hypertonic reference, then $0 = -p' + H_a(du'/dz)$, so that the initial osmotic pressure is

$$p' = H_a \frac{du'}{dz}. \quad (B2)$$

Under the same bath concentration c^* , if v is the solid matrix displacement measured from the equilibrium configuration and σ is the applied stress, then

$$v = u - u', \quad (B3)$$

and

$$\sigma = -p + H_a \frac{\partial v}{\partial z} + H_a \frac{\partial u'}{\partial z} = -(p - p') + H_a \frac{\partial v}{\partial z}, \quad (B4)$$

i.e.,

$$\sigma = -(p - p') + H_a \varepsilon, \quad (B5)$$

where ε is the matrix strain relative to the free swelling configuration at c^* . For this one-dimensional problem, the biphasic aggregate modulus H_A is given by the relation $\sigma = H_A \varepsilon$. Thus, inserting this expression into Eq. (B5) yields:

$$H_A \varepsilon = -(p - p') + H_a \varepsilon, \quad (B6)$$

and the relation between H_A and H_a is given by

$$H_A = H_a - \frac{p - p'}{\varepsilon}. \quad (B7)$$

Here the pressure p and p' are given by:

$$p = RT(2c^- + c^F - 2c^*), \quad (B8)$$

$$p' = RT(2c_o^- + c_o^F - 2c^*), \quad (B9)$$

where

$$c^- = \frac{-c^F + \sqrt{(c^F)^2 + 4c^{*2}}}{2}, \quad (B10)$$

Table 1 Values of H_A ($\varepsilon = -0.05$)

$c^* = 0.15 \text{ M}$	$H_a(\text{MPa})$						
	$\phi_o^w = 0.85$	0.1	0.2	0.3	0.4	0.5	0.6
c_o^F	0.05	0.126	0.226	0.326	0.426	0.526	0.626
mEq/ml	0.10	0.199	0.299	0.399	0.499	0.599	0.699
	0.15	0.309	0.409	0.509	0.609	0.709	0.809
	0.20	0.445	0.545	0.645	0.745	0.845	0.945

Table 2 Values of H_A ($\varepsilon = -0.10$)

$c^* = 0.15 \text{ M}$	$H_a(\text{MPa})$						
	$\phi_o^w = 0.85$	0.1	0.2	0.3	0.4	0.5	0.6
c_o^F	0.05	0.128	0.228	0.328	0.428	0.528	0.628
mEq/ml	0.10	0.209	0.309	0.409	0.509	0.609	0.709
	0.15	0.329	0.429	0.529	0.629	0.729	0.829
	0.20	0.476	0.576	0.676	0.776	0.876	0.976

$$c_o^- = \frac{-c_o^F + \sqrt{(c_o^F)^2 + 4c^{*2}}}{2}, \quad (B11)$$

and

$$c^F = c_o^F / (1 + \varepsilon / \phi_o^w), \quad (B12)$$

with c_o^F and ϕ_o^w denoting FCD and porosity at $\varepsilon = 0$ respectively.

Thus, the biphasic aggregate modulus H_A depends on the triphasic aggregate modulus as well as the following variables: c_o^F , c^* , ϕ_o^w , and ε . Tables 1 and 2 give the values of H_A as a function of H_a and c_o^F , for two imposed strains ($\varepsilon = -0.05$ and -0.10) at $c^* = 0.15 \text{ M}$.

References

- [1] Bachrach, N. M., Valhmu, W. B., Stazzone, E. J., Ratcliffe, A., Lai, W. M., and Mow, V. C., 1995, "Changes in Proteoglycan Synthesis of Chondrocytes in Articular Cartilage Are Associated With the Time-Dependent Changes in Their Mechanical Environment," *J. Biomech.*, **28**, pp. 1561–1569.
- [2] Brighton, C. T., Jenson, L., Pollack, S. R., Tolin, B. S., and Clark, C. C., 1989, "Proliferative and Synthetic Response of Bovine Growth Plate Chondrocytes to Various Capacitatively Coupled Electric Fields," *J. Orthop. Res.*, **7**, pp. 759–765.
- [3] Freeman, P. M., Natarajan, R. N., Kimura, J. H., and Andriachi, T. P., 1994, "Chondrocyte Cells Respond Mechanically to Compressive Loads," *J. Orthop. Res.*, **12**, pp. 311–320.
- [4] Gray, M. L., Pizzanelli, A. M., Grodzinsky, A. J., and Lee, R. C., 1988, "Mechanical and Physicochemical Determinants of the Chondrocyte Biosynthetic Response," *J. Orthop. Res.*, **6**, pp. 777–792.
- [5] Guilak, F. A., Meyers, B. C., Ratcliffe, A., and Mow, V. C., 1994, "The Effect of Matrix Compression on Proteoglycan Metabolism in Articular Cartilage Explants," *Osteoarthritis Cartilage*, **2**, pp. 91–101.
- [6] Guilak, F. A., Sah, R. L., and Setton, L. A., 1997, "Physical Regulation of Cartilage Metabolism," in: *Basic Orthopaedic Biomechanics*, Mow V. C., and Hayes, W. C., eds., Lippincott-Raven Pubs., Philadelphia, pp. 179–207.
- [7] Hall, A. C., Urban, J. P. G., and Gehl, K. A., 1991, "The Effects of Hydrostatic Pressure on Matrix Synthesis in Articular Cartilage," *J. Orthop. Res.*, **9**, pp. 1–10.
- [8] Kim, Y. J., Bonassar, L. J., and Grodzinsky, A. J., 1995, "The Role of Cartilage Streaming Potential, Fluid Flow and Pressure in the Stimulation of Chondrocyte Biosynthesis During Dynamic Compression," *J. Biomech.*, **28**, pp. 1055–1066.
- [9] Lafeber, F., Veldhuijzen, J. P., Vanroy, A. M., Huber-Bruning, O., and Bijlsma, J. W. J., 1992, "Intermittent Hydrostatic Compressive Force Stimulates Exclusively the Proteoglycan Synthesis of Osteoarthritic Human Cartilage," *Br. J. Rheumatol.*, **31**, pp. 437–442.
- [10] MacGinitie, L. A., Gluzband, Y. A., and Grodzinsky, A. J., 1994, "Electric Field Stimulation Can Increase Protein Synthesis in Articular Cartilage Explants," *J. Orthop. Res.*, **12**, pp. 151–160.
- [11] Sah, R. L., Kim, Y. J., Doong, L.-Y. H., Grodzinsky, A. J., Plaas, A. H. K., and Sandy, J. D., 1989, "Biosynthetic Response of Cartilage Explants to Dynamic Compression," *J. Orthop. Res.*, **7**, pp. 619–636.
- [12] Sah, R. L., Grodzinsky, A. J., Plaas, A. H. K., and Sandy, J. D., 1992, "Effects of Static and Dynamic Compression on Matrix Metabolism in Cartilage Explants," in: *Articular Cartilage and Osteoarthritis*, Kuettner, K. E., Schleyerback, R., Peyron, J. G., and Hascall, V. C., eds., Raven Press, New York, pp. 373–392.
- [13] Schneiderman, R. D., Kevet, A., and Maroudas, A., 1986, "Effects of Mechanical and Osmotic Pressure on the Rate of Glycosaminoglycan Synthesis in the Human Adult Femoral Head Cartilage: An in Vitro Study," *J. Orthop. Res.*, **4**, pp. 393–408.
- [14] Wang, N., Butler, J. P., and Ingber, D. E., 1993, "Mechano-transduction Across the Cell Surface and Through the Cytoskeleton," *Science*, **260**, pp. 1124–1127.
- [15] Valhmu, W. B., Stazzone, E. J., Bachrach, N. M., Saed-Nejad, F., Fischer, S. G., Mow, V. C., and Ratcliffe, A., 1998, "Constant Compressive Loading of Articular Cartilage Induces a Transient Stimulation of Aggrecan Gene Expression," *Arch. Biochem. Biophys.*, **353**, pp. 29–36.

- [16] Comper, W. D., 1996, *Extracellular Matrix*, **2**, Harwood Academic Publishers, Australia.
- [17] Mow, V. C., and Ratcliffe, A., 1997, "Structure and Function of Articular Cartilage and Meniscus," in: *Basic Orthopaedic Biomechanics*, Mow, V. C., and Hayes, W. C., eds., Lippincott-Raven Pubs., Philadelphia, pp. 113–177.
- [18] Muir, H., 1983, "Proteoglycans as Organizers of the Extracellular Matrix," *Biochem. Soc. Trans.*, **11**, pp. 613–622.
- [19] Bassett, C. A. L., and Pawluk, R. J., 1972, "Electrical Behavior of Cartilage During Loading," *Science*, **178**, pp. 982–983.
- [20] Buschmann, M. D., and Grodzinsky, A. J., 1995, "A Molecular Model of Proteoglycan-Associated Electrostatic Forces in Cartilage Mechanics," *ASME J. Biomech. Eng.*, **117**, pp. 180–192.
- [21] Chen, A. C., Nguyen, T. T., and Sah, R. L., 1997, "Streaming Potentials During the Confined Compression Creep Test of Normal and Proteoglycan-Depleted Cartilage," *Ann. Biomed. Eng.*, **25**, pp. 269–277.
- [22] Frank, E. H., and Grodzinsky, A. J., 1987, "Cartilage Electromechanics. I. Electrokinetic Transduction and the Effects of Electrolyte pH and Ionic Strength," *J. Biomech.*, **20**, pp. 615–627.
- [23] Frank, E. H., and Grodzinsky, A. J., 1987, "Cartilage Electromechanics. II. A Continuum model of Cartilage Electrokinetics and Correlation With Experiments," *J. Biomech.*, **20**, pp. 629–639.
- [24] Frank, E. H., Grodzinsky, A. J., Koob, T. J., and Eyre, D. R., 1987, "Streaming Potentials: A Sensitive Index of Enzymatic Degradation in Articular Cartilage," *J. Orthop. Res.*, **5**, pp. 497–508.
- [25] Eisenberg, S. R., and Grodzinsky, A. J., 1985, "Swelling of Articular Cartilage and Other Connective Tissues: Electromechanochemical Forces," *J. Orthop. Res.*, **3**, pp. 148–159.
- [26] Grodzinsky, A. J., Lipshitz, H., and Glimcher, M. J., 1978, "Electromechanical Properties of Articular Cartilage During Compression and Stress Relaxation," *Nature (London)*, **275**, pp. 448–450.
- [27] Gu, W. Y., Lai, W. M., and Mow, V. C., 1993, "Transport of Fluid and Ions Through a Porous-Permeable Charged-Hydrated Tissue, and Streaming Potential Data on Normal Bovine Articular Cartilage," *J. Biomech.*, **26**, pp. 709–723.
- [28] Lee, R. C., Frank, E. H., Grodzinsky, A. J., and Roylance, D. K., 1981, "Oscillatory Compressional Behavior of Articular Cartilage and Its Associated Electromechanical Properties," *ASME J. Biomech. Eng.*, **103**, pp. 280–292.
- [29] Lotke, P. A., Black, J., and Richardson, S. J., 1974, "Electromechanical Properties in Human Articular Cartilage," *J. Bone Jt. Surg.*, **56A**, pp. 1040–1046.
- [30] Maroudas, A., 1968, "Physicochemical Properties of Cartilage in the Light of Ion Exchange Theory," *Biophys. J.*, **8**, pp. 575–595.
- [31] Maroudas, A., 1975, "Swelling Pressure Versus Collagen Tension in Normal and Degenerate Articular Cartilage," *Nature (London)*, **260**, p. 808.
- [32] Maroudas, A., 1979, "Physicochemical Properties of Articular Cartilage," in: *Adult Articular Cartilage*, 2nd ed., Freeman, M. A. R., ed., Pitman Medical Pub., Kent, U.K., pp. 215–290.
- [33] Maroudas, A., Muir, H., and Wingham, J., 1969, "The Correlation of Fixed Negative Charge With Glycosaminoglycan Content of Human Articular Cartilage," *Biochim. Biophys. Acta*, **177**, pp. 492–500.
- [34] Hascall, V. C., and Hascall, G. K., 1983, "Proteoglycans," in: *Cell Biology of Extracellular Matrix*, Hay, E. D., ed., Plenum Press, pp. 39–63.
- [35] Lai, W. M., Hou, J. S., and Mow, V. C., 1991, "A Triphasic Theory for Swelling and Deformation Behavior of Articular Cartilage," *ASME J. Biomech. Eng.*, **113**, pp. 245–258.
- [36] Gu, W. Y., Lai, W. M., and Mow, V. C., 1998, "A Mixture Theory for Charged Hydrated Soft Tissues Containing Multi-electrolytes: Passive Transport and Swelling Behaviors," *ASME J. Biomech. Eng.*, **120**, pp. 169–180.
- [37] Mow, V. C., Kuei, S. C., Lai, W. M., and Armstrong, C. G., 1980, "Biphasic Creep and Stress Relaxation of Articular Cartilage in Compression: Theory and Experiments," *ASME J. Biomech. Eng.*, **102**, pp. 73–84.
- [38] Donnan, F. G., 1924, "The Theory of Membrane Equilibria," *Chem. Rev.*, **1**, pp. 73–90.
- [39] Helfferich, F., 1962, *Ion Exchange*, McGraw-Hill, New York.
- [40] Lai, W. M., Ateshian, G. A., Sun, D. N., and Mow, V. C., 1999, "The Electrical Environment of Chondrocytes in Normal and OA Cartilage: Streaming Potential vs. Nernst Potential," *Proc. ASME Bioengng. Conf., Y. C. Fung 80th Anniversary Biomechanics Symposium*, ASME BED-Vol. 42, pp. 135–136.
- [41] Katchalsky, A., and Curran, P. F., 1975, *Non Equilibrium Thermodynamics in Biophysics*, Harvard University Press, Boston, MA.
- [42] Mow, V. C., Wang, C. B., and Hung, C. T., 1999, "The Extracellular Matrix, Interstitial Fluid and Ions as a Mechanical Signal Transducer in Articular Cartilage," *Osteoarthritis Cartilage*, **7**, pp. 41–58.
- [43] Huyghe, J. M., and Janssen, J. D., 1997, "Quadruphasic Mechanics of Swelling Incompressible Porous Media," *Int. J. Eng. Sci.*, **35**, pp. 793–802.
- [44] Hasse, R., 1969, *Thermodynamics of Irreversible Processes*, Addison-Wesley, Reading, MA (also, Dover reprinted ed., 1990).
- [45] Holmes, M. H., and Mow, V. C., 1990, "The Nonlinear Characteristics of Soft Gels and Hydrated Connective Tissues in Ultrafiltration," *J. Biomech.*, **23**, pp. 1145–1156.
- [46] Lai, W. M., and Mow, V. C., 1980, "Drag-Induced Compression of Articular Cartilage During Permeation Experiment," *Biorheology*, **17**, pp. 111–123.
- [47] Ateshian, G. A., Warden, W. H., Kim, J. J., Grelsamer, R. P., and Mow, V. C., 1997, "Finite Deformation Biphasic Material Properties of Bovine Articular Cartilage From Confined Compression Experiments," *J. Biomech.*, **30**, pp. 1157–1164.
- [48] Holmes, M. H., Lai, W. M., and Mow, V. C., 1985, "Singular Perturbation Analysis of the Nonlinear, Flow-Dependent, Compressive Stress Relaxation Behavior of Articular Cartilage," *ASME J. Biomech. Eng.*, **107**, pp. 206–218.
- [49] Lai, W. M., Mow, V. C., and Roth, V., 1981, "Effects of Nonlinear Strain-Dependent Permeability and Rate of Compression on the Stress Behavior of Articular Cartilage," *ASME J. Biomech. Eng.*, **103**, pp. 61–66.
- [50] Mow, V. C., Ateshian, G. A., Lai, W. M., and Gu, W. Y., 1998, "Effects of Fixed Charges on the Stress-Relaxation Behavior of Hydrated Soft Tissues in a Confined Compression Problem," *Int. J. Solids Struct.*, **35**, pp. 4945–4962.
- [51] Sun, D. N., Gu, W. Y., Guo, X. E., Lai, W. M., and Mow, V. C., 1999, "A Mixed Finite Element Formulation of Triphasic Mechano-Electrochemical Theory for Charged, Hydrated Biological Soft Tissues," *Int. J. Numer. Methods Eng.*, **45**, pp. 1375–1402.
- [52] Ateshian, G. A., Lai, W. M., Gu, W. Y., and Mow, V. C., 1998, "Ionic Polarization in Charged Hydrated Soft Tissues," *Advances in Bioengineering*, ASME BED-Vol. 39, pp. 253–254.
- [53] Armstrong, C. G., and Mow, V. C., 1982, "Variations in the Intrinsic Mechanical Properties of Human Cartilage With Age, Degeneration and Water Content," *J. Bone Jt. Surg.*, **64A**, pp. 88–94.
- [54] Overbeek, J. T. G., 1961, "The Donnan Equilibrium," *Prog. Biophys. Mol. Biol.*, **6**, pp. 57–126.
- [55] Setton, L. A., Elliot, D. M., and Mow, V. C., 1999, "Altered Mechanics of Cartilage with Osteoarthritis: Human OA and Animal Model of Joint Degeneration," *Osteoarthritis Cartilage*, **7**, pp. 2–14.